

Corrosion of cordierite ceramics by sodium sulphate at 1000° C

ROBERT BIANCO*, NATHAN JACOBSON
NASA Lewis Research Center, Cleveland, Ohio 44135, USA

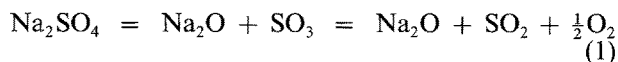
The corrosion of a sintered cordierite ($2\text{MgO} \cdot 2\text{Al}_2\text{O}_3 \cdot 5\text{SiO}_2$) ceramic by sodium sulphate (Na_2SO_4) – a common combustion condensate – was investigated at 1000° C. Laboratory tests with thin films of $\text{Na}_2\text{SO}_4/\text{O}_2$ and $\text{Na}_2\text{SO}_4/1\% \text{SO}_2\text{-O}_2$ were performed. In the $\text{Na}_2\text{SO}_4/\text{O}_2$ case, the cordierite reacted to form NaAlSiO_4 . After several hours of corrosion, the Na_2SO_4 appeared to induced surface cracks in the cordierite. In the $\text{Na}_2\text{SO}_4/1\% \text{SO}_2\text{-O}_2$ case, other dissolution reactions occurred. The material was also tested in a burner rig with No. 2 Diesel fuel and 2 ppm sodium. The corrosion process was similar to that observed in the $\text{Na}_2\text{SO}_4/\text{O}_2$ furnace tests, with more severe attack occurring.

1. Introduction

Cordierite ($2\text{MgO} \cdot 2\text{Al}_2\text{O}_3 \cdot 5\text{SiO}_2$ or MAS) ceramics are well known to have several desirable high temperature properties including a low coefficient of thermal expansion, stability in air at elevated temperatures, and a high melting point [1, 2]. For these reasons, they are being considered for a variety of combustion applications.

Recently cordierite was selected for the regenerator in the ceramic, advanced gas turbine (AGT) engine [3]. This material is produced in the form of a honeycomb. The resultant high surface area allows maximum heating of the incoming air. Under conditions similar to these, Na_2SO_4 may form by the reaction of ingested salt and/or sodium impurities in the fuel with sulphur impurities [4]. Thus, the cordierite ceramic regenerator in the AGT is a possible site for hot corrosion [5]. Fig. 1 is a view of a section of this material (Corning Glass Works, Corning, New York, USA.), which was placed in a crucible with a small amount of Na_2SO_4 at the bottom and heated for 24 h in air at 1000° C. Subsequent metallographic examination of this material revealed that the Na_2SO_4 collected on the walls and corners of the cells. A close up of the affected zone shows a rough interface between the Na_2SO_4 and cordierite, suggesting some reaction.

The hot corrosion process has been extensively studied for metals [6] and more recently for silicon-based ceramics [7, 8]. The key component from Na_2SO_4 is sodium oxide formed as follows



A high $P(\text{SO}_3)$ sets a low Na_2O activity (acidic salt) and a low $P(\text{SO}_3)$ sets a high Na_2O activity (basic salt).

The cordierite system is considerably different from previously studied metal or silicon-based ceramic systems. First, the reaction may occur with three oxides, each at less than unit activity. Second, oxidation is not

a part of the reaction process; hence, the kinetics of the reaction cannot be followed with simple weight-gain techniques.

There is only limited information on the molten salt corrosion of cordierite. Brooks and Morrell [9] examined the behaviour of cordierite in a burner rig containing large amounts of fuel impurities. At 900 and 1100° C only limited corrosion occurred, but at 1400° C extensive attack of the ceramic occurred. The larger field of refractory corrosion by slags is related to this study [10]. In this case, corrosion is controlled by both mass transport away from the refractory and the solubility limits of the refractory in the slag. In the case of alumina, grain boundaries have been found to be preferential sites of corrosion [11]. Cook [12] has examined another complex refractory – potassium aluminosilicate – in a slag. In an oxidizing environment, only limited dissolution occurred.

The purpose of this paper is to examine the molten salt corrosion of MAS with particular regard to combustion applications. Laboratory thin film studies were performed, with both $\text{Na}_2\text{SO}_4/\text{O}_2$ and a more acidic system – $\text{Na}_2\text{SO}_4/1\% \text{SO}_2\text{-O}_2$. In addition, burner rig tests were performed.

2. Experimental procedure

For the purposes of this study, dense coupons of cordierite were used. Pure cordierite is extremely difficult to sinter and hence small amounts of additional oxides are added to promote sintering [1]. The material used to produce the commercially manufactured honeycomb shown in Fig. 1 contains less than 1 w/o each of Fe_2O_3 , TiO_2 , Na_2O and CaO [2]. For this study a powder (Ferro Corporation, Cleveland, Ohio, USA.) of the composition 13.7 w/o MgO , 52.0 w/o SiO_2 , 31.7 w/o Al_2O_3 and 2.0 w/o BaO was used for coupon fabrication. Subsequent experiments indicated that the additives did not play a major role in corrosion. An optimum processing schedule was

*Present address: Department of Materials Science and Engineering, Ohio State University, Columbus, Ohio 43210, USA.

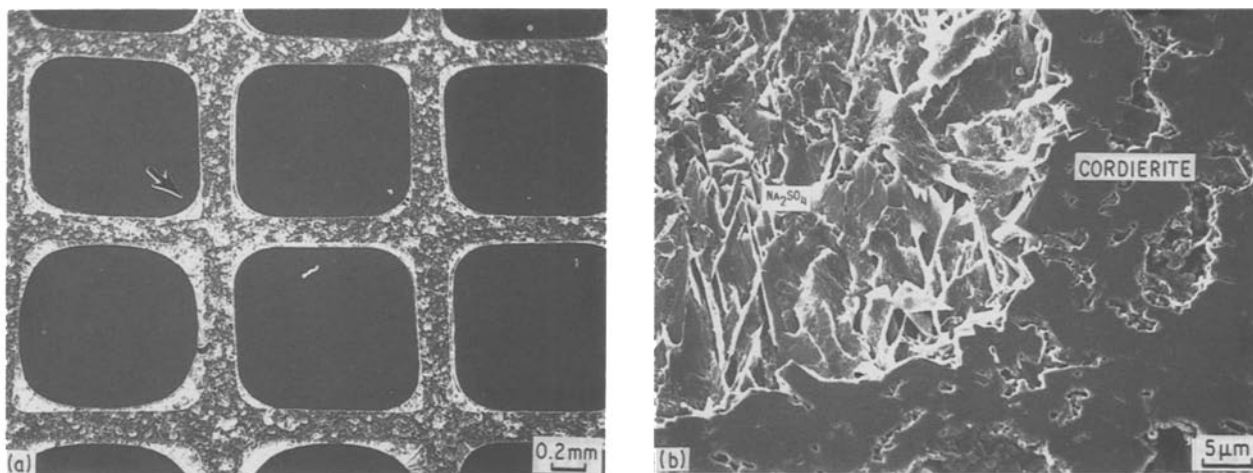


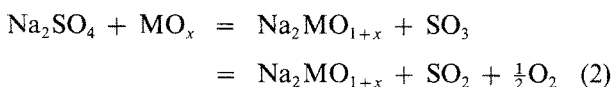
Figure 1 Honeycomb cordierite corroded in $\text{Na}_2\text{SO}_4/\text{O}_2$ for 24 h. (a) Overall view. (b) Closeup of marked section.

developed based on cold pressing into 2.14×0.5 cm discs at 15000 lb (1 lb = 0.454 kg) without a binder. These discs were then sintered at 1100°C for 15.5 h. This produced a material with a density measured by the Archimedes method to be $2.566 \pm 0.011 \text{ g cm}^{-3}$, which is about 2.7% higher than the theoretical density [13] of 2.499 g cm^{-3} . This discrepancy may be due to the formation of a small amount of glass phase. X-ray diffraction of a pellet showed only cordierite with two unknown peaks – possibly residual BaO or some other additional sintering oxide. Examination of a polished surface with an optical and an electron microscope showed no evidence of a second phase.

These discs were then cut in half, heated to about 200°C on a hot plate, and coated with an aqueous salt solution from an airbrush. A coating of $2.50 \pm 0.25 \text{ mg Na}_2\text{SO}_4 \text{ cm}^{-2}$ was used. Samples were then placed in a horizontal furnace with gas flowing at about $100 \text{ cm}^3 \text{ min}^{-1}$ STP. For some experiments pure oxygen was used; for other experiments a platinum catalysed 1% $\text{SO}_2\text{-O}_2$ mixture was used. For this 1%

$\text{SO}_2\text{-O}_2$ mixture, a $P(\text{SO}_3)$ of $6.5 \times 10^{-3} \text{ atm}$ at 1000°C was calculated.

As mentioned, standard thermogravimetric techniques could not be used to follow the kinetics of this reaction. Therefore other techniques had to be found to follow the chemical changes induced by this reaction. One technique which involves a pulsed fluorescent SO_2 analyser [14]. This instrument (Thermo Electron Corporation, Hopkinton, Massachusetts, USA) is used with $\text{Na}_2\text{SO}_4/\text{O}_2$ experiments only and is sensitive to the ppm of SO_2 released by the following type of reaction



Here MO_x is a metal oxide, such as SiO_2 . At 1000°C , most of the SO_3 decomposes to SO_2 , which is then detected by the SO_2 analyser. For comparison purposes, a platinum coupon coated with Na_2SO_4 was run under the same conditions. Very little SO_2 was released as shown in Fig. 3.

Another technique to follow the kinetics of the corrosion process was chemical analysis of the corrosion products. In this approach, different specimens are run for various times. In each case the corrosion products are cleanly removed from the substrate, using a solvent which dissolves the corrosion products, but not the substrate. In the case of SiC [7], a 10% HF solution fit these requirements. However, the

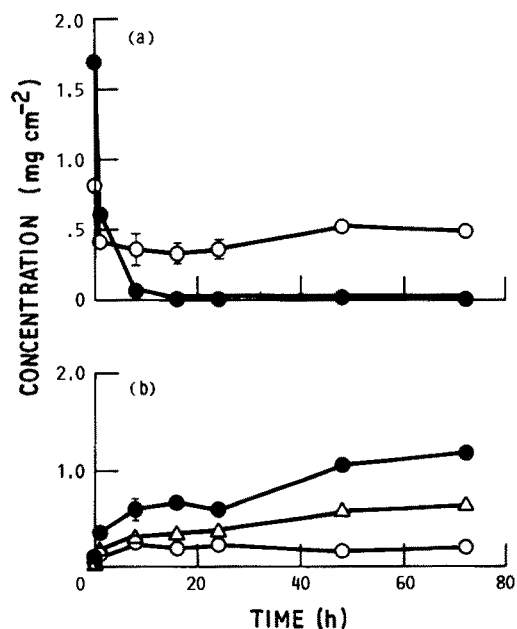


Figure 2 Reaction kinetics of cordierite + $\text{Na}_2\text{SO}_4/\text{O}_2$ as indicated by chemical analysis. (a) Na (O), SO_4 (●). (b) Mg (Δ), Al (●), Si (O).

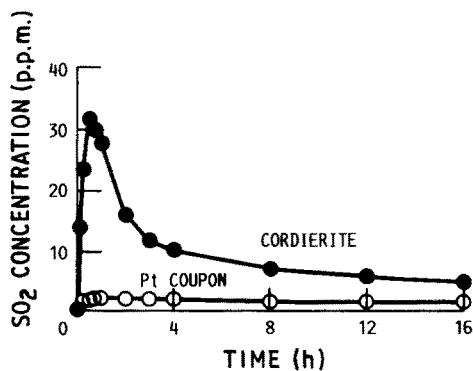


Figure 3 Evolution of SO_2 for cordierite corroded in $\text{Na}_2\text{SO}_4/\text{O}_2$.

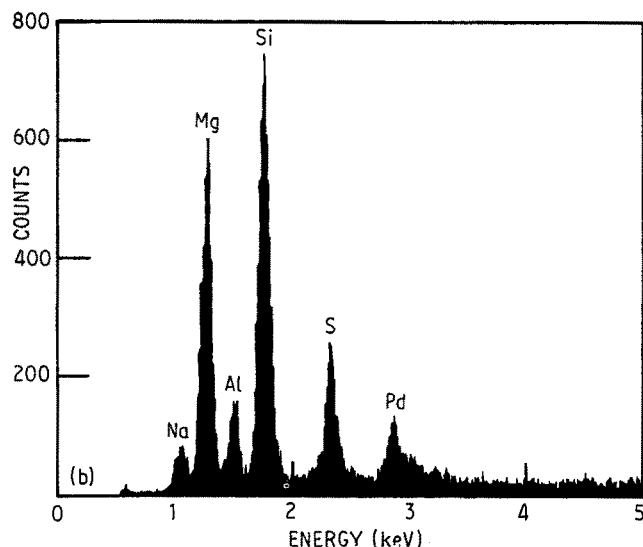
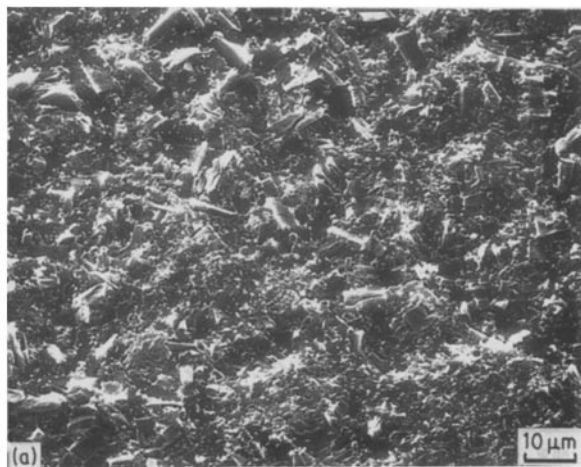


Figure 4 Cordierite + Na₂SO₄/O₂, 2 h. (a) Surface view. (b) EDS data for crystallite in (a).

same solution attacked the cordierite substrate. Hot water did not attack the substrate, but only partially removed the corrosion products. The literature on refractory corrosion of slags suggested that an HCl solution might work for cordierite [11]. Several cordierite coupons were immersed in warm 50% HCl for 2 h and essentially no attack occurred. However 50% HCl did remove nearly all of the corrosion products. The resulting solution was analysed for sodium, silicon, magnesium and aluminium by atomic emission spectroscopy. Analysis for SO₄²⁻ were performed by precipitation to BaSO₄ and an X-ray fluorescence technique [15]. The stripped substrate appeared somewhat silicon rich as compared to the starting material according to Energy Dispersive Spectroscopy. The analyses may therefore underestimate the amount of silicon.

The products were also examined with X-ray diffraction (XRD), which is sensitive only to the crystalline products and would not pick up any amorphous products common in these types of reactions. Surface morphologies were determined with the scanning electron microscope (SEM). Cross-sections were prepared by sputtering a layer of gold and then electroplating a thick layer of copper over the sample. The specimens were then mounted in epoxy and polished with diamond paste. Kerosene was used as a lubricant and



Figure 5 Surface view – cordierite + Na₂SO₄:O₂, 24 h.

trichlorethane was used as a solvent to preserve any water soluble phases. These cross sections were then examined in an electron microprobe, which was equipped with a wavelength dispersive spectrometer so that X-ray maps of oxygen, sodium, magnesium, aluminium, silicon and barium could be obtained.

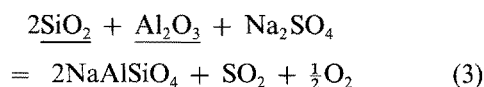
Some specimens were prepared using larger rectangular dies in the form of bars roughly 2 × 0.5 × 0.25 cm³. These were run in a burner rig at 1000°C at 4 atm total pressure and a velocity of 310 ft sec⁻¹ (1 ft = 0.3048 m). The burner rig has been described in detail elsewhere [8]. No. 2 diesel fuel with ~0.5% sulphur was used and 2 ppm sodium was injected into the flame as NaCl. The total run for three specimens lasted for 40 h with one brief cool down period after 32 h. After the run, the specimens were analysed using the techniques described above.

3. Results and discussion

3.1. Laboratory studies

The Na₂SO₄ with a flowing oxygen environment simulated the atmosphere encountered in a combustion environment with a low sulphur fuel [8]. In this case, the reaction kinetics were followed both with chemical analyses and the SO₂ analyser, as shown in Figs 2 and 3.

In Fig. 2a, the decrease in SO₄²⁻ concentration after eight hours indicates that the Na₂SO₄ has decomposed and the sodium reacted to form part of the corrosion scale. The results from the SO₂ analyser (Fig. 3) are consistent with this decomposition, suggesting a reaction of the type given in Equation 2. After only 1 h of corrosion, NaAlSiO₄ was detected by XRD, suggesting the following reaction



The underlined compounds exhibit less than unit activity as components in the solid cordierite solution. The chemical analysis kinetic curves for magnesium, aluminium and silicon (Fig. 2b) show the incorporation of these elements into the corrosion scale. As noted, the silicon analyses may be low, since a silicon rich film remained on the cordierite after leaching.

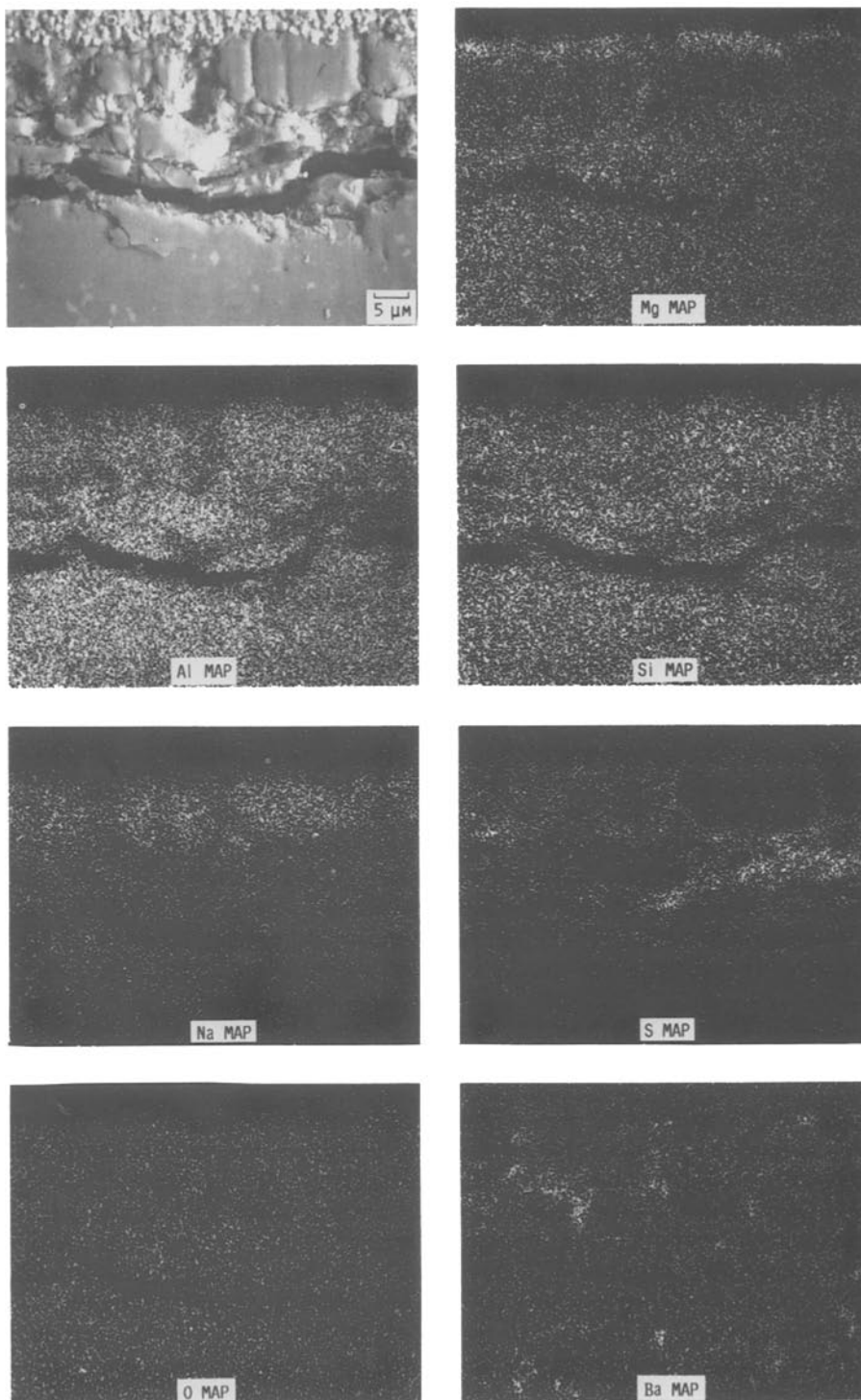


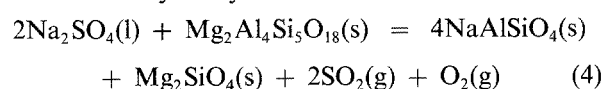
Figure 6 Polished cross section and associated dot maps of cordierite + Na₂SO₄/O₂, 72 h.

The morphologies of the corrosion products are helpful in understanding the reaction. In the first hour of reaction, surface views showed a solidified Na₂SO₄ layer, consistent with chemical analysis and XRD results. As the reaction continued, small crystallites emerged from the melt, as shown in Fig. 4a. The EDS data (Fig. 4b) for these crystallites showed only magnesium and silicon and a somewhat lower level of aluminium than the cordierite starting material. This suggests a Mg₂SiO₄ product, but there was no clear evidence of this compound in the XRD results.

As the reaction continued, the Na₂SO₄(l) was less prevalent on the surface and the crystallites became more dominant as shown in Fig. 5. Fig. 6 shows a polished cross section with associated X-ray dot maps after 72 h of reaction. The large crystallites of

NaAlSiO₄ that were observed in XRD, are seen. The region between the NaAlSiO₄ grains contains some sulphur, suggesting some remaining Na₂SO₄. The upper layer contains primarily magnesium, silicon and oxygen, which again suggests Mg₂SiO₄. Note that this layer is very small compared to the larger NaAlSiO₄ grains. The dominant X-ray pattern indicated the cordierite substrate with the NaAlSiO₄ grains producing a weaker pattern. Thus the thin Mg₂SiO₄ layer did not produce a clear pattern.

On basis of the above observations, the overall reaction is very likely



The solid reactants and products in this equation are

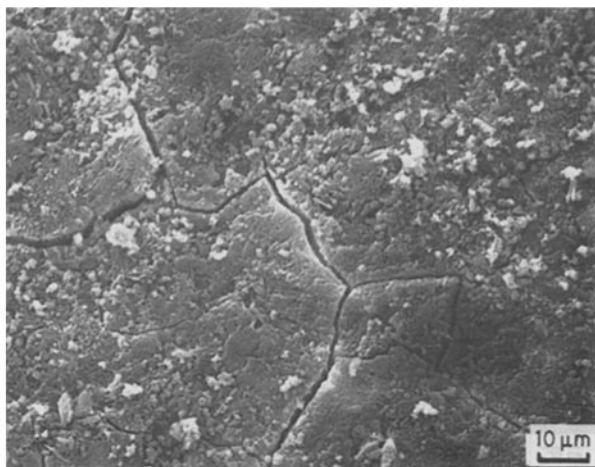


Figure 7 Surface view of cordierite + Na₂SO₄/O₂, 24 h, scale removed with HCl.

all silicate structures and therefore the reaction may only involve some simple structural changes. Using thermodynamic data from several sources [16–18], a free energy change of +27.74 kcal mol⁻¹ was calculated for the above reaction. The positive free energy change indicates that the reaction is not favourable as written. However, with a flowing oxygen environment, the reaction should proceed to the right, as indicated by the evolved SO₂ and product analyses. Taking the above condensed phase compounds to have unity activity and the oxygen pressure to be 1 atm, a P(SO₂) of 4.2 × 10⁻³ atm can be calculated. If this amount or more is in the atmosphere above the Na₂SO₄, reaction 4 is suppressed.

Next, consider the physical changes induced by corrosion. In all the microstructures examined, there was evidence of cracking (Figs 4 to 6). The polished cross-section (Fig. 6) suggests that these cracks extend below the corrosion product scale and into the cordierite substrate. Fig. 7 is a surface view of the material corroded for 24 h after the corrosion scale had been removed by the HCl treatment. The clear presence of substrate cracks indicates that they result from the corrosion process. The physical mechanism by which

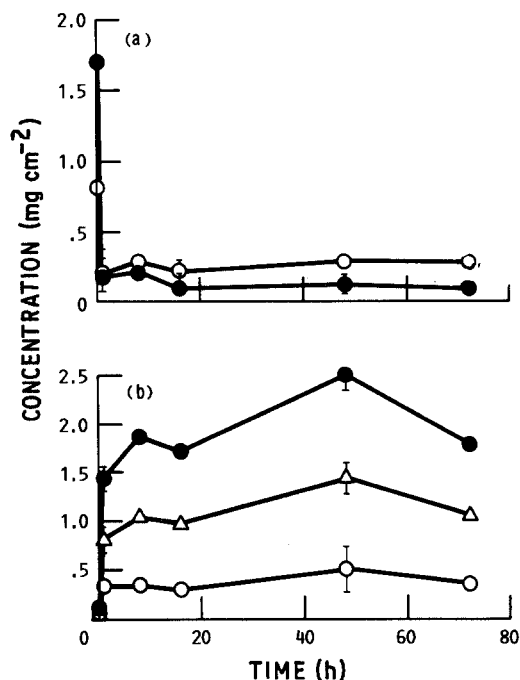


Figure 8 Reaction kinetics of cordierite + Na₂SO₄/0.01 SO₃-O₂, as indicated by chemical analysis. (a) Na (○), SO₄ (●). (b) Mg (Δ), Al (●), Si (○).

this occurs is not clear. Perhaps sodium devitrifies a glassy grain boundary phase in the cordierite, leading to a new phase and corresponding volume change, or Na₂SO₄ may penetrate into the cordierite and create the cracks upon cooling.

Reaction 4 indicates that the pressure of SO₂ above the deposit would be expected to play an important role in the corrosion process. Furthermore, higher sulphur fuels can create a high P(SO₂) above a salt deposit in a combustion environment [19]. To examine this further, laboratory tests were performed using a 1% SO₂-O₂ atmosphere. The kinetic curves for this reaction are shown in Figs 8a and b. Note that SO₄⁻ does not decompose entirely in this situation. Note also the higher levels of aluminium, magnesium and silicon than for the Na₂SO₄/O₂ case. Surface morphology observations also showed differences. The surface contained several droplets of Na₂SO₄ which were

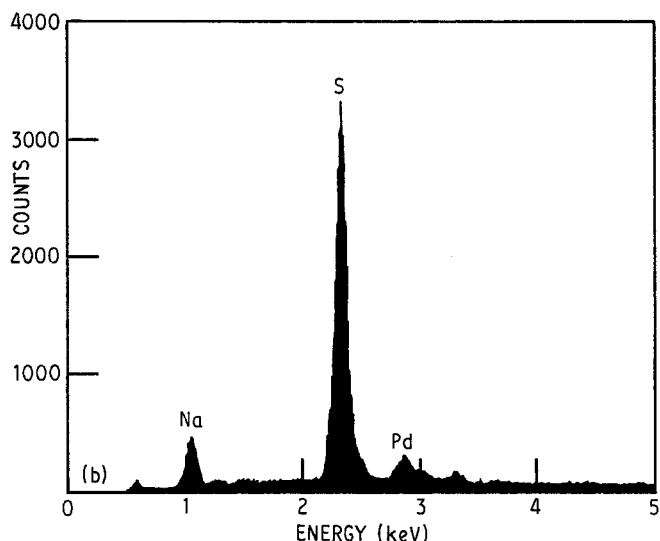
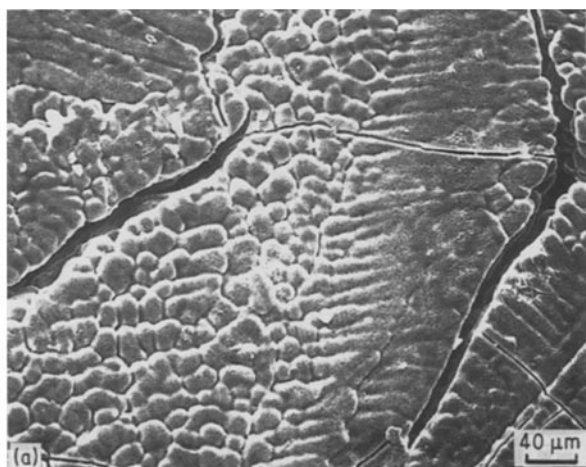


Figure 9 Cordierite corroded in Na₂SO₄/1% SO₂-O₂ for 16 h. Na₂SO₄ droplet remaining on surface. (a) Surface view. (b) Associated EDS data.

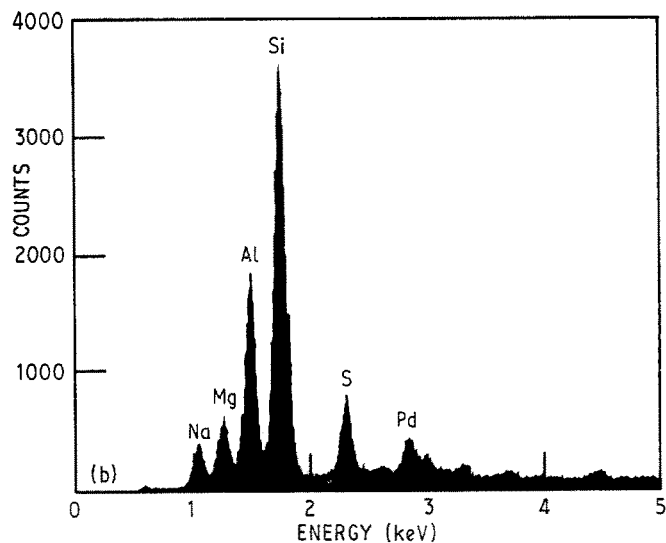
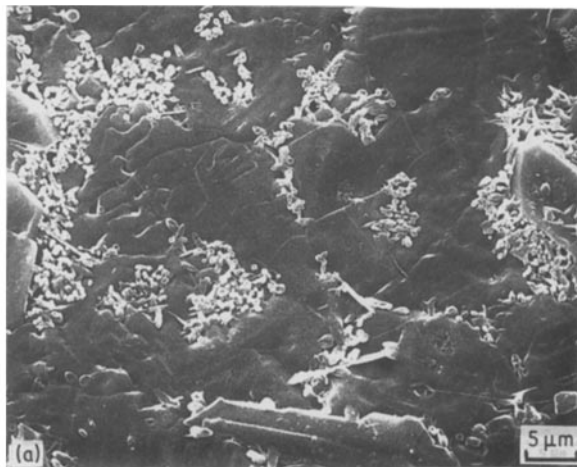
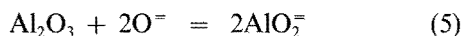


Figure 10 Cordierite corroded in $\text{Na}_2\text{SO}_4/1\% \text{SO}_2\text{-O}_2$ for 16 h. Representative appearance of surface away for Na_2SO_4 droplet. (a) Surface view. (b) Associated EDS data.

approximately 1 to 2 mm in diameter. A portion of one of these droplets and associated EDS spectra is shown in Fig. 9. Other portions of the surface appeared smooth and contained sodium, magnesium, aluminium, silicon and sulphur, as shown in Fig. 10. These portions may be a glassy melt containing these species.

From Reaction 1, a $P(\text{SO}_2)$ of 1×10^{-2} sets the $a(\text{Na}_2\text{O})$ to be 7.1×10^{-14} at 1000°C . Consider the three constituent oxides of cordierite. Pure SiO_2 has a calculated threshold $a(\text{Na}_2\text{O})$ for dissolution [19] of 1×10^{-10} at 1000°C . This value would shift for the lower activity of SiO_2 in the cordierite solution, but it is unlikely that it would shift enough to allow basic SiO_2 dissolution to occur to any large extent. Pure alumina exhibits a solubility minimum at $a(\text{Na}_2\text{O})$ equal to 4×10^{-16} at 900°C [20]. These conditions are then on the basic side of the alumina dissolution curve



There is only limited information on magnesia. However, it is a basic oxide and therefore would be expected to undergo only acidic dissolution



XRD showed primarily cordierite for specimens corroded at 16 and 72 h, with no strong evidence for NaAlSiO_4 , as observed in the $\text{Na}_2\text{SO}_4/\text{O}_2$ case. However, there were a few very weak peaks which corresponded to the JCPDS card for $1.01\text{Na}_2\text{O} \cdot \text{Al}_2\text{O}_3 \cdot 1.68\text{SiO}_2 \cdot 1.73\text{H}_2\text{O}$. Small amounts of this compound formed either in local regions of the melt where the activity of Na_2O was high or else upon cool down.

In summary attack of cordierite by $\text{Na}_2\text{SO}_4/\text{O}_2$ appears to occur by Reaction 4. The observed dependence on $P(\text{SO}_2)$ supports this. In an oxygen atmosphere, formation of NaAlSiO_4 is clearly favoured. In a 1% $\text{SO}_2\text{-O}_2$ atmosphere, other dissolution routes may be more important.

3.2. Burner rig studies

The burner rig provides a more realistic view of corrosion than the furnace tests. Three specimens were run

in a burner rig under the conditions discussed previously. The specimens seen in Fig. 11 clearly show a deposit and possible corrosion product. Chemical analyses of these deposits (Table I) indicated the presence of Na_2SO_4 and other compounds with generally the same composition found in the furnace tests. A polished cross-section (Fig. 12) shows the same features as observed in the furnace tests with $\text{Na}_2\text{SO}_4/\text{O}_2$ (Fig. 6). The layer on the top appears to be Mg_2SiO_4 , with larger underlying regions of NaAlSiO_4 . The calculated $P(\text{SO}_2)$ in this case is 3.9×10^{-4} atm [19], indicating Reaction 4 would be favourable.

There are again numerous cracks in this material. The overall appearance of the cross-section is similar to that observed by Brooks and Morrell [9] for cordierite run in a similar burner. Both the cracks and amount of corrosion product in the burner test are larger than those observed in the furnace test, due to greater severity of the burner rig test.

4. Conclusions

The corrosion behaviour of cordierite in Na_2SO_4 at 1000°C has been discussed. Furnace corrosion tests with thin films of Na_2SO_4 produced NaAlSiO_4 and



Figure 11 Cordierite corroded in a 4 atm burner rig for 40 h at 1000°C .

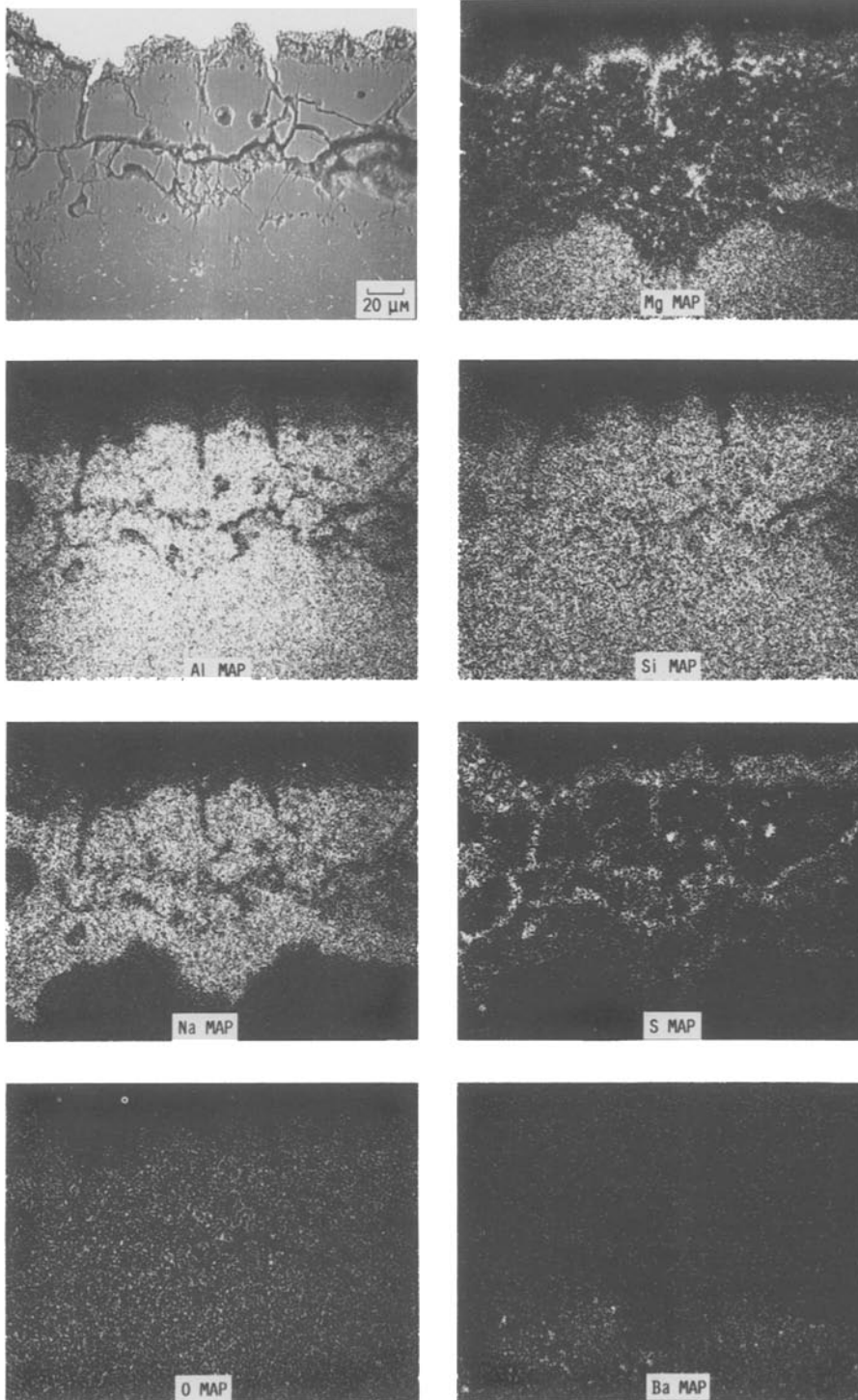


Figure 12 Polished cross-section and associated dot maps for the second specimen in Fig. 11.

probably Mg_2SiO_4 . In addition corrosion appeared to induce cracking in the cordierite. Furnace corrosion tests with thin films of $\text{Na}_2\text{SO}_4/1\% \text{SO}_2\text{-O}_2$ promoted other dissolution routes for MgO and Al_2O_3 . Burner rig tests with No. 2 diesel fuel produced similar morphologies to the laboratory furnace tests, but with more extensive attack. In combustion applications, it

appears oxide dissolution is limited, but corrosion cracking may be a problem.

Acknowledgement

The authors would like to thank Professor R. A. Rapp for his helpful comments.

TABLE I Burner rig results

Species	Amount (mg cm^{-2})
Na	0.87 ± 0.04
SO_4^-	0.59 ± 0.41
Al	0.96 ± 0.16
Si	0.12 ± 0.01
Mg	0.34 ± 0.07

References

1. R. MORRELL, *Proc. Brit. Ceram. Soc.* **28** (1978) 53.
2. I. M. LACHMAN, R. D. BAGLEY and R. M. LEWIS, *Amer. Ceram. Soc. Bull.* **60** (1981) 202.
3. G. L. BOYD, J. R. KIDWELL and D. M. KREINER, in "Proceedings of the Twenty-Fourth Automotive Technology Development Contractors' Coordination Meeting" (Society of Automotive Engineers, Warrendale, PA, 1986) pp. 115-135.
4. F. J. KOHL, C. A. STEARNS and G. C. FRYBURG,

- in "Metal-Slag-Gas Reactions and Process" (The Electrochemical Society, Princeton, New Jersey, 1975) pp. 649-654.
5. T. STRANGMAN, Private Communication.
 6. R. A. RAPP, *Corrosion-NACE* **42** (1986) 568.
 7. N. S. JACOBSON, *J. Amer. Ceram. Soc.* **69** (1986) 74.
 8. N. S. JACOBSON, C. A. STEARNS and J. L. SMIALEK, *Adv. Ceram. Mater.* **1** (1986) 154.
 9. S. BROOKS and R. MORRELL, in "Environmental Degradation of High Temperature Materials", Vol. 2 (Institute of Metallurgists, London, 1980) pp. 3/21-3/25.
 10. W. D. KINGERY, H. K. BOWEN and D. R. UHLMANN, "Introduction to Ceramics", 2nd Edn (Wiley, New York, 1976) pp. 407-413.
 11. B. N. SAMADDAR, W. D. KINGERY and A. R. COOPER, Jr., *J. Amer. Ceram. Soc.* **47** (1964) 249.
 12. L. P. COOK, in "19th Symposium on Engineering Aspects of Magnetohydrodynamics", edited by M. H. Scott (University of Tennessee Space Institute, Tullahoma, Tennessee, 1981) pp. 15.3.1-15.3.6.
 13. *Handbook of Chemistry and Physics*, 39th Edn, edited by C. D. Hodgeman (Chemical Rubber Company, Cleveland, Ohio, 1957).
 14. G. C. FRYBURG, F. J. KOHL, C. A. STEARNS and W. L. FIELDER, *J. Electrochem. Soc.* **129** (1982) 571.
 15. C. L. LUKE, *Anal. Chim. Acta.* **43** (1968) 245.
 16. I. BARIN and O. KNACKE, "Thermomechanical Properties of Inorganic Substances" (Springer-Verlag, New York, 1973).
 17. *Idem*, "Thermomechanical Properties of Inorganic Substances, Supplement" (Springer-Verlag, New York, 1977).
 18. H. C. HELGESON, J. M. DELANY, H. W. NESBITT and D. K. BIRD, *Amer. J. Sci.* **278-A** (1978) 1.
 19. N. S. JACOBSON, *Oxid. of Metals* **31** (1989) 91.
 20. P. D. JOSE, D. K. GUPTA and R. A. RAPP, *J. Electrochem. Soc.* **132** (1985) 735.

*Received 31 May
and accepted 13 September 1988*